Nano-TiO_2, ultrasound and sequential nano-TiO_2/ultrasonic degradation of N-acetyl-para-aminophenol from aqueous solution

Olushola S. Ayanda, Simphiwe M. Nelana, Leslie F. Petrik and Eliazer B. Naidoo

ABSTRACT

The application of nano-TiO_2 as adsorbent combined with ultrasound for the degradation of N-acetyl-para-aminophenol (AAP) from aqueous solution was investigated. The nano-TiO_2 was characterized by means of powder X-ray diffraction (XRD), scanning electron microscopy (SEM), transmission electron microscopy (TEM), energy dispersive spectroscopy (EDS), and attenuated total reflection–Fourier transform infrared spectroscopy (ATR-FTIR). Experimental results revealed that the adsorption of AAP by nano-TiO_2 fitted the pseudo-second-order kinetic model, the equilibrium could be explained by the Freundlich isotherm and the treatment process is exothermic. The optimum removal efficiency of AAP (128.89 mg/g (77.33%)) was achieved at pH 4 when 0.03 g of nano-TiO_2 was mixed with 50 mL of 100 mg/L AAP aqueous solution at ambient temperature, 60 min contact time, and a stirring speed of 120 rpm. Ultrasound at 20 kHz and pH 3 was favorable and it resulted in 52.61% and 57.43% removal efficiency with and without the addition of nano-TiO_2, respectively. The degradation of AAP by ultrasound followed by nano-TiO_2 treatment resulted in approximately 99.50% removal efficiency. This study showed that a sequential ultrasound and nano-TiO_2 treatment process could be employed for the removal of AAP or other emerging water and wastewater contaminants.

Key words | adsorption, degradation, N-acetyl-para-aminophenol, pharmaceuticals, TiO_2, ultrasound

Olushola S. Ayanda (corresponding author)
Simphiwe M. Nelana
Eliazer B. Naidoo
Department of Chemistry,
Vaal University of Technology,
Vanderbijlpark 1900,
South Africa
E-mail: *osayanda@gmail.com*

Olushola S. Ayanda
Nanoscience Research, Department of Industrial Chemistry,
Federal University Oye Ekiti,
P.M.B 373, Oye Ekiti, Ekiti State,
Nigeria

Leslie F. Petrik
Environmental and Nano Sciences Group, Department of Chemistry,
University of the Western Cape,
Private Bag X17, Bellville 7535,
South Africa

INTRODUCTION

Pharmaceuticals such as analgesics, antibiotics, antiepileptics, etc., are not completely removed during wastewater treatment. Pharmaceuticals are usually present in the treatment effluents, contaminating waterways and public water supplies all over the world; they are among important emerging water contaminants (Moussavi *et al.* 2016). The release of pharmaceuticals into water bodies has led to their accumulation which adversely affects the ecosystem as well as causing prolonged effects on human health. Pharmaceuticals are intended to preserve their chemical structure long enough to exert their therapeutic effect. This property, as well as the continuous use of these drugs, enables pharmaceutical products to persist in the environment for a long period of time (Isariebel *et al.* 2009). N-acetyl-para-aminophenol (AAP; acetaminophen or paracetamol) is a drug component that has been used to reduce inflammation and relieve fever and pain by blocking enzymes and proteins associated with pain. It is regarded as one of the most widely prescribed pharmaceuticals around the world (Galhetas *et al.* 2014; Zavala & Estrada 2016). It was estimated in 1998 that 3.2×10^9 AAP tablets were consumed in the UK (Xagoraraki *et al.* 2008). Stackelberg *et al.* (2004), Gomez *et al.* (2007), Ternes (1998), and Gros *et al.* (2006) reported the occurrence of AAP in surface water, raw wastewater,

doi: 10.2166/wh.2017.145

treated wastewater, and treated drinking water, respectively. Zavala & Estrada (2016) identified the toxic effects of AAP on microorganisms in aquatic systems. Therefore, there is a need to treat water and wastewater containing pharmaceutical products in order to improve water quality and protect human health.

Moussavi *et al.* (2016) investigated the adsorption of AAP on double-oxidized graphene oxide. The authors reported that the maximum adsorption capacity of AAP (704 mg/g) was obtained at $pH \leq 8$, the adsorption data was well fitted by the pseudo-second-order kinetic and Langmuir equilibrium model. Isariebel *et al.* (2009) evaluated the influence of operating conditions of the ultrasound process on the degradation of AAP and levodopa. The authors reported that the ultrasonic degradation of these drugs follows a pseudo-first-order reaction kinetics and the best results were obtained with 574 kHz ultrasonic frequency. The ultrasonic degradation of AAP and naproxen in the presence of powdered activated carbon and biochar adsorbents has been reported by Im *et al.* (2014). The authors described that the degradation of pollutants in aqueous phase by ultrasound occurs by the formation, growth, and implosive collapse of bubbles in a liquid; this involves some reaction pathways such as pyrolysis inside the bubble and hydroxyl radical-mediated reactions at the bubble–liquid interface and/or in the liquid bulk (Isariebel *et al.* 2009).

TiO_2 is a promising oxide that has been commonly used in photocatalytic applications due to its unique strong oxidizing power, high photostability, and redox selectivity. TiO_2 exists in rutile (tetragonal), anatase (tetragonal), and brookite (orthorhombic) forms. It can be synthesized by chemical impregnation, hydrothermal method, direct oxidation of $TiCl_4$, metal organic chemical vapor deposition method, physical vapor deposition, etc. (Haider *et al.* 2015). Well dispersed TiO_2 nanoparticles (nano-TiO_2) with fine sizes are promising in many applications (Vijayalakshmi & Rajendran 2012) such as in pigments, catalytic supports, photocatalysts, and adsorbents for the remediation of contaminated water and wastewater. Several investigations such as chemical (Hiremath *et al.* 2006), electrochemical (Arredondo Valdez *et al.* 2012), adsorption (Galhetas *et al.* 2014), Fenton (Basavaraju *et al.* 2011), photocatalysis (Yang *et al.* 2009; Aguilar *et al.* 2011), ozonation (Andreozzi *et al.* 2003), ultrasound (Isariebel *et al.* 2009), UV (Ratpukdi 2014) and the combined methods have been carried out on the removal of AAP in aqueous solutions. Nevertheless, partial degradation of AAP was achieved rather than total degradation; besides, many of these techniques require high voltage or incessant chemical feeds which increase the operational cost (Zavala & Estrada 2016). Previous research studies have shown that the integration of different treatment systems enhances treatment efficiency as well as reduces cost. An advanced oxidation process such as ultrasound is regarded as a pretreatment method in an integrated system. Therefore, the integration of ultrasound treatment process and adsorption will be useful to take advantage of the methods and to minimize the drawback of the two methods.

The objective of this study is to investigate the potential of nano-TiO_2, ultrasound and a combined/sequential nano-TiO_2/ultrasound for the remediation of a model aqueous solution of AAP. The influence of various operating conditions on the removal efficiency of AAP was investigated as well as the modeling of the kinetics, equilibrium, and thermodynamic studies. The importance of this treatment technique is its low cost and it could be employed in a scaled-up water treatment process for large volumes containing organic and inorganic pollutants.

MATERIALS AND METHODS

Reagents

Titanium(IV) oxide nanopowder, 21 nm primary particle size, and AAP (>99%) were supplied by Sigma-Aldrich. The nano-TiO_2 was chosen based on its unique chemical and biological inertness, high surface area, and low cost of production. Stock solution containing 1,000 mg/L AAP was prepared by dissolving 1.0 g of AAP in 1,000 mL of deionized water and the made up solution was stored in the dark at 4°C. Working solutions were prepared daily by serial dilution. Hydrochloric acid (HCl) and sodium hydroxide (NaOH) were used to adjust the pH of AAP solutions during the study of the influence of pH on the degradation efficiency.

Characterization of nano-TiO_2

The mineral phase identification of the nano-TiO_2 was conducted by X-ray diffraction (Siemens D8 Advance Bruker XRD). The morphology of nano-TiO_2 was obtained by scanning electron microscopy (SEM; Nova Nano SEM 230) and transmission electron microscopy (TEM; FEI Tecnai G^2 20). Energy dispersive spectroscopy (EDS) was used to study the elemental composition of nano-TiO_2 and the infrared spectrum was obtained by Perkin Elmer Universal attenuated total reflection–Fourier transform infrared (UATR-FTIR) Spectrum Two™ spectrometer.

Experimental design

Adsorption of N-acetyl-para-aminophenol with nano-TiO_2

The adsorption of AAP was achieved by mixing a range of nano-TiO_2 (0.01–0.05 g) at ambient temperature with 50 mL of 100 mg/L AAP aqueous solution (pH 5.66), which was stirred at 120 rpm for 10 min. After the optimization of the nano-TiO_2 dosage, a 0.03 g of nano-TiO_2 was mixed with 50 mL of 100 mg/L AAP aqueous solution and stirred at 120 rpm for different contact times ranging from 15 to 100 min. The results obtained on the influence of contact times were used for the kinetic investigation. The equilibrium study was examined at AAP concentration ranging from 6.25 to 100 mg/L. The pH (adjusted with 0.05 M HCl and NaOH) was investigated at pH 3–8.37, while the thermodynamic parameters were obtained by treating 100 mg/L AAP aqueous solution with nano-TiO_2 at 295 K to 343 K.

Degradation of N-acetyl-para-aminophenol with ultrasound

A 100 mL of 100 mg/L AAP solution was placed in a 250 mL beaker and sonicated (Misonix Ultrasonic Liquid Processors Sonicator S-4000) at 20 kHz ultrasonic frequency for 60 min. This followed the optimization of pH and time on the ultrasound degradation efficiency of AAP. After the optimization of pH and time, AAP aqueous solution was sonicated at 20, 40, 80, and 100 kHz ultrasonic frequencies with or without nano-TiO_2.

Samples were taken (from the ultrasonic reactor), filtered through 0.45 µm Biofil syringe filter (as the case when nano-TiO_2 was involved) after the elapsed time and analyzed by a UV/visible spectrophotometer (model: Nicolet Evolution 100) at a wavelength of 245 nm (Isariebel *et al.* 2009). All experiments were conducted in triplicate. The percentage of AAP removal and the amount (mg) of AAP per g nano-TiO_2 were calculated using Equations (1) and (2), respectively:

$$\%\text{AAP removal} = \frac{AAP_o - AAP_e}{AAP_o} \times 100 \quad (1)$$

$$q_e = \frac{AAP_o - AAP_e}{W_{nTiO_2}} \times V_{AAP} \quad (2)$$

where AAP_o and AAP_e (mg/L) are the initial and equilibrium concentration of the AAP aqueous solution, respectively, W_{nTiO2} (g) is the mass of nano-TiO_2, and V_{AAP} (mL) is the volume of the AAP solution. The experimental runs and operational conditions are given in Table 1.

RESULTS AND DISCUSSION

Nano-TiO_2 characterization

The morphological study of nano-TiO_2 by SEM (Figure 1(a)) and TEM (Figure 2(b)) indicated regular spherical shaped particles of nano-TiO_2. The EDS (Figure 1(b)) as an attachment of the scanning electron microscope showed that the nano-TiO_2 is made up of C (20.53 ± 4.39%), O (42.82 ± 5.06%), and Ti (36.65 ± 3.85%). From Figure 2(a), it was observed that the diffraction peaks of nano-TiO_2 that appeared in the pattern corresponded to the anatase and rutile TiO_2 phase with good crystallinity.

Anatase (JCPDS Card no. 21-1272) peaks are found at 2θ values of 25.3°, 36.9°, 37.8°, 48.1°, 53.9°, 55.06°, 62.7°, 68.8°, 70.3°, 75.0°, and 82.7°; these correspond to (101), (103), (004), (200), (105), (211), (204), (116), (220), (215), and (224) crystal planes. Rutile (JCPDS Card no. 21-1276)

Table 1 | Experimental runs and operational conditions

Adsorption by Nano-TiO_2		**Experimental conditions**						
Run	**Aim**	**Nano-TiO_2 dosage (g)**	**Concentration of AAP (mg/L)**	**Volume of AAP (mL)**	**Contact time (min)**	**pH**	**Temperature (K)**	**Stirring speed (rpm)**
1	Influence of nano-TiO_2 dosage	0.01–0.05	100	50	10	5.66	Ambient	120
2	Influence of contact time	0.03	100	50	15–100	5.66	Ambient	120
3	Influence of initial AAP concentration	0.03	6.25–100	50	60	5.66	Ambient	120
4	Influence of pH	0.03	100	50	60	3–8.37	Ambient	120
5	Influence of temperature	0.03	100	50	60	5.66	295–343	120

Ultrasound degradation

Run	**Aim**	**Ultrasonic frequency (kHz)**	**Concentration of AAP (mg/L)**	**Volume of AAP (mL)**	**Time (min)**	**pH**	**Stirring speed (rpm)**
1	Influence of pH	20	100	100	60	3–8	180
2	Influence of ultrasound time	20	100	100	10–60	3	180
3	Influence of ultrasonic frequency	20–100	100	100	60	3	180

Combined nano-TiO_2/ultrasound degradation

Run	**Aim**	**Ultrasonic frequency (kHz)**	**Concentration of AAP (mg/L)**	**Volume of AAP (mL)**	**Time (min)**	**pH**	**Stirring speed (rpm)**	**Nano-TiO_2 dosage (g)**
1	Influence of pH	20	100	100	60	3–8	180	0.03
2	Influence of ultrasound time	20	100	100	10–60	3	180	0.03
3	Influence of ultrasonic frequency	20–100	100	100	60	3	180	0.03

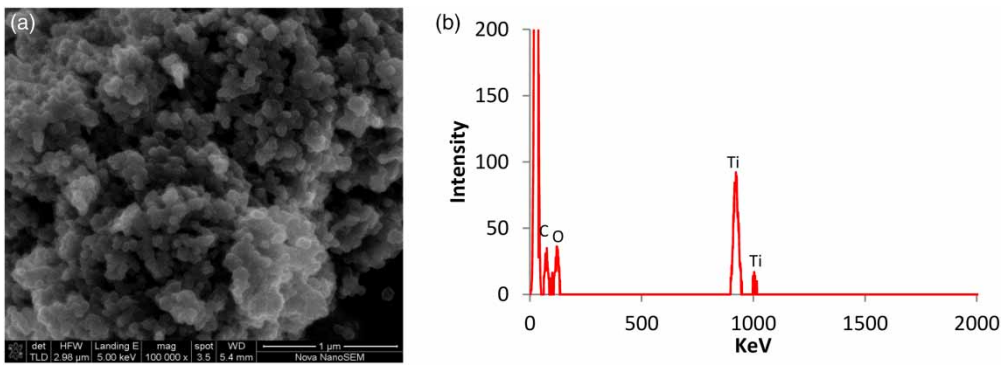

Figure 1 | SEM image (a) and EDS (b) of nano-TiO_2.

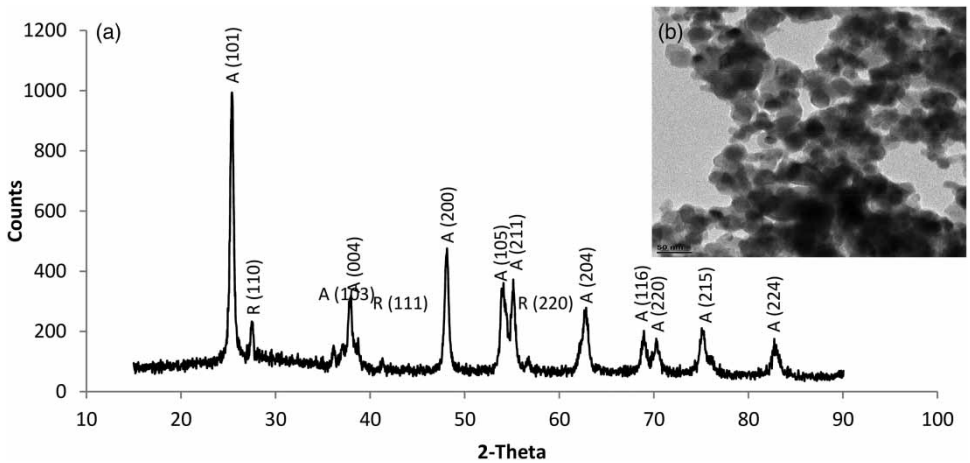

Figure 2 | XRD (a) and TEM (b) of nano-TiO_2. A, anatase TiO_2; R, rutile TiO_2.

peaks are found at 2θ values of 27.4°, 41.2°, and 56.6°; these correspond to crystal planes of (110), (111), and (220). The anatase peaks were dominant; consequently, the nano-TiO_2 that was used in this study was mainly of anatase form.

The FTIR spectrum of nano-TiO_2 (Figure 3) showed very weak absorption in the frequency region of 1,638.46 cm^{-1}; the absorption at 1,638.46 cm^{-1} corresponds to Ti-O-Ti vibrations. Adsorption bands which may correspond to Ti-O bonding were obtained below the 400 cm^{-1} regions (400–350 cm^{-1}).

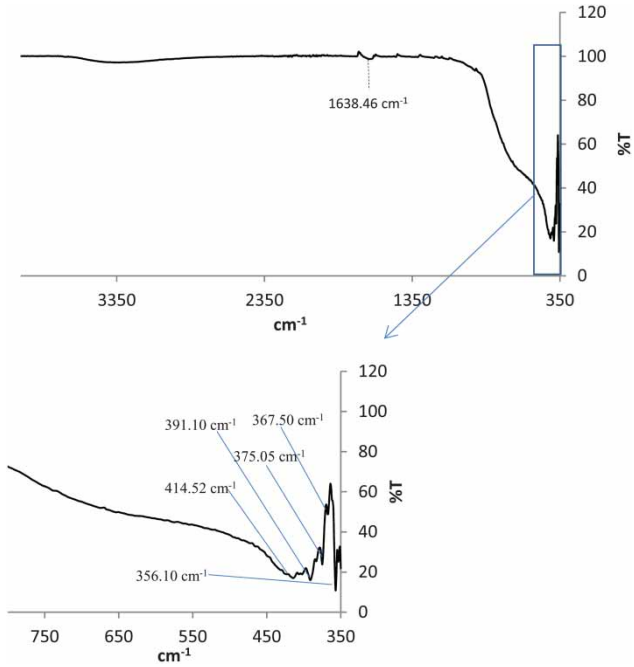

Figure 3 | FTIR spectrum of nano-TiO_2.

Adsorption capacity of AAP by nano-TiO_2

Figure 4 shows the results on the influence of nano-TiO_2 dosage on the treatment of 100 mg/L AAP. The results showed an initial rapid removal of AAP (46.09 mg/g) within 10 min with 0.01 g nano-TiO_2. The increase of the nano-TiO_2 dosage from 0.01 g to 0.03 g brought about equilibration after which the percentage of AAP removed decreases as the nano-TiO_2 dosage increased from 0.03 g to 0.05 g. The aggregation of nano-TiO_2 particles in AAP

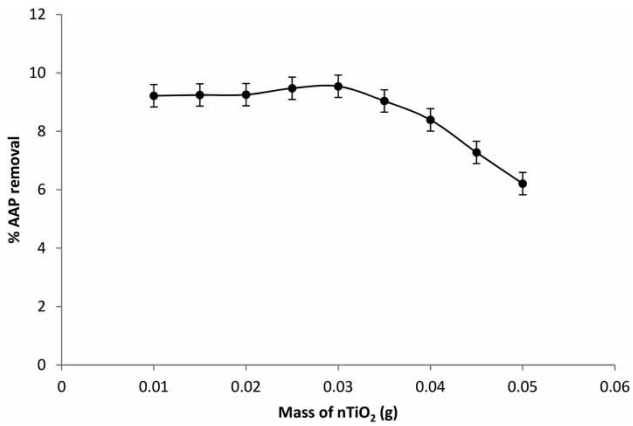

Figure 4 | Influence of nano-TiO_2 dosage. Experimental conditions: concentration of AAP: 100 mg/L; vol. of AAP aqueous solution: 50 mL; contact time: 10 min; stirring speed: 120 rpm; pH of solution 5.66; ambient temperature.

aqueous solution at these dosages (0.03–0.05 g) might possibly limit the available active site of nano-TiO_2 and consequently lead to the reduction of the removal of AAP. This is supported by Pettibone *et al.* (2008) who mentioned that the aggregation of nano-TiO_2 plays a significant role in the amount of surface area available for adsorption and that aggregation negatively impacts the activity of nanoparticles. A 0.03 g dosage of nano-TiO_2 was chosen and maintained for further experiments.

Likewise, a rapid adsorption of AAP (77.23 mg/g) within 15 min was observed with 0.03 g nano-TiO_2. The removal efficiency sharply increased to 112.81 mg/g in 60 min, which may be credited to a larger surface area of nano-TiO_2 being available with time for the AAP molecules. The percentage removal of AAP, however, slightly reduced from 67.69% to 60.67% as the contact time was further increased from 60 to 100 min (Figure 5). Thus, 60 min contact time was maintained for further experiments. The slight reduction in the amount of AAP adsorbed at higher contact times could be attributed to the saturation of the active sites of the nano-TiO_2 by the AAP.

The kinetics of the nano-TiO_2 AAP treatment process were investigated by applying the pseudo-first and pseudo-second-order kinetic models as represented in Equations (3) and (4), respectively:

$$\log_{10}(q_e - q_t) = \log q_e + \frac{k_1}{2.303}t \quad (3)$$

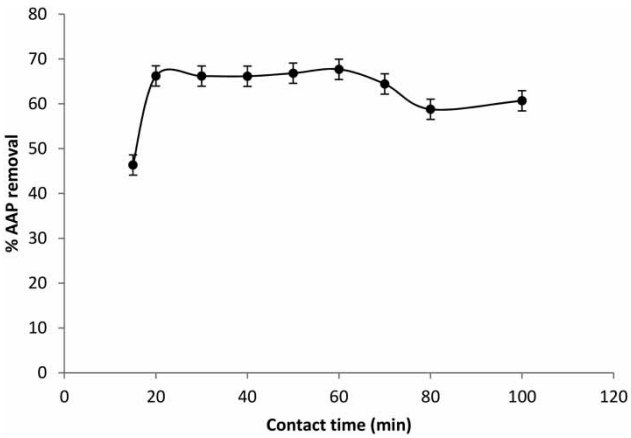

Figure 5 | Influence of contact time. Experimental conditions: concentration of AAP: 100 mg/L; vol. of AAP aqueous solution: 50 mL; nano-TiO_2 dosage: 0.03 g; stirring speed: 120 rpm; pH of solution 5.66; ambient temperature.

$$\frac{t}{q_t} = \frac{1}{k_2 q_e^2} + \frac{t}{q_e} \quad (4)$$

where q_e is the equilibrium amount of AAP adsorbed per unit mass of nano-TiO_2 (mg/g), t is time (min), q_t is the amount of AAP adsorbed per unit mass of nano-TiO_2 at time t (mg/g), k_1 and k_2 obtained from Figures 6 and 7 are the pseudo-first and pseudo-second-order adsorption rate constants, respectively.

The kinetic information obtained from fitting the pseudo-first and pseudo-second-order kinetic models with the experimental data are summarized in Table 2. As seen in Table 2, the experimental data had better fitness (higher R^2 value; $R^2 = 0.9848$) with the pseudo-second-order model than with the pseudo-first-order kinetic model. Moreover, the experimental adsorption capacity q_e (113.98 mg/g) was close to the calculated q_e (102.04 mg/g), confirming the high correlation of AAP adsorption by nano-TiO_2 to the pseudo-

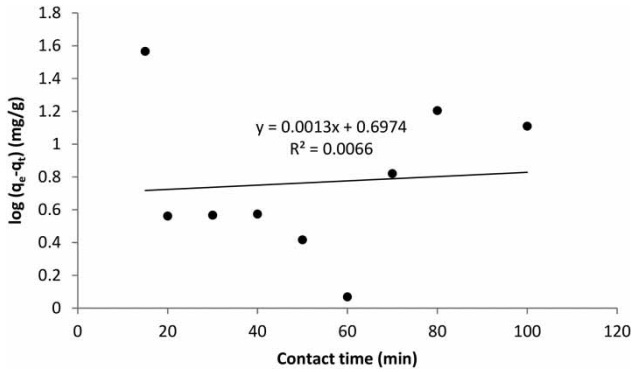

Figure 6 | Pseudo-first-order kinetic plot.

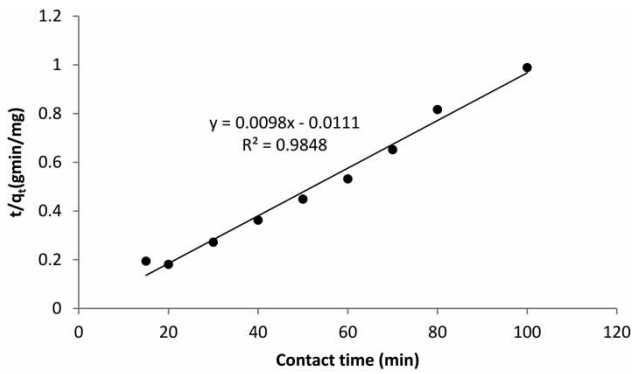

Figure 7 | Pseudo-second-order kinetic plot.

Table 2 | Equilibrium and kinetic parameters for the removal of AAP by nano-TiO_2

Equilibrium models					
Langmuir model			**Freundlich model**		
q_m (mg/g)	K_L (L/mg)	R^2	K_F (mg/g (L/mg)$^{1/n}$)	n	R^2
1,250	2.76×10^{-3}	0.028	3.5653	1.025	0.9545
Kinetic models					
Pseudo-first-order			**Pseudo-second-order**		
k_1(min^{-1})	q_e(mg/g)	R^2	k_2(g/mg/min)	q_e(mg/g)	R^2
2.99×10^{-3}	4.982	0.0066	8.66×10^{-3}	102.041	0.9848

second-order model. This implies that chemisorption is the rate limiting step, and that the AAP and nano-TiO_2 were affecting the adsorption process under the investigated conditions. Chen *et al.* (2015) and Moussavi *et al.* (2016) likewise reported that the removal of pharmaceuticals (sulfamethoxazole, ciprofloxacin, AAP) from aqueous solutions by graphene oxide followed the pseudo-second-order kinetic model.

The results of the influence of the initial AAP concentration are depicted in Figure 8. Figure 8 shows that the adsorption capacity of AAP initially increased from 61.94% at AAP concentration of 6.25 mg/L to 74.38% at AAP concentration of 25 mg/L; it slightly reduced from 73.38% to 66.64% when the AAP concentration was increased to 40 mg/L after which the adsorption capacity tended towards equilibrium. On the contrary, the equilibrium adsorption capacity increased from 6.45 mg/g to 112 mg/g when the initial AAP concentration was increased from 6.25 mg/L to 100 mg/L. The increase could be as a result of the enhancement of mass transfer rates due to a higher AAP gradient concentration at a higher initial AAP concentration, leading to the uptake of more AAP molecules per nano-TiO_2 mass unit.

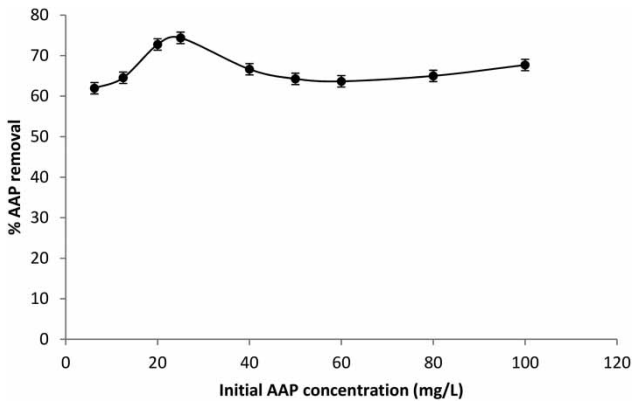

Figure 8 | Influence of initial AAP concentration. Experimental conditions: vol. of AAP aqueous solution: 50 mL; nano-TiO_2 dosage: 0.03 g; contact time: 60 min; stirring speed: 120 rpm; pH of solution 5.66; ambient temperature.

The equilibrium study of the nano-TiO_2 treatment process was considered by applying the linearized form of the Langmuir (Equation (5)) and Freundlich (Equation (6)) models to the experimental data presented in Figure 8:

$$\frac{AAP_e}{AAP_a} = \frac{1}{q_m K_L} + \frac{AAP_e}{q_m} \tag{5}$$

$$\log AAP_a = logK_F + \frac{1}{n}\log AAP_e \tag{6}$$

where AAP_e, AAP_a, q_m, and n are the equilibrium concentration of AAP solution (mg/L), the amount of AAP adsorbed per unit mass of nano-TiO_2 (mg/g), Langmuir constant representing adsorption capacity (mg/g), and the number of layers, respectively. K_L and K_F from Figures 9 and 10 are the Langmuir (L/mg) and Freundlich (mg/g (L/mg)$^{1/n}$) constants, respectively.

The equilibrium parameters obtained from fitting the Langmuir and Freundlich equilibrium models are also summarized in Table 2. Based on Table 2, the equilibrium data had better fitness (higher R^2 value; $R^2 = 0.9545$) with the Freundlich model than with the Langmuir equilibrium model, which implies that AAP uptake occurs as a multilayer onto a heterogeneous nano-TiO_2 surface.

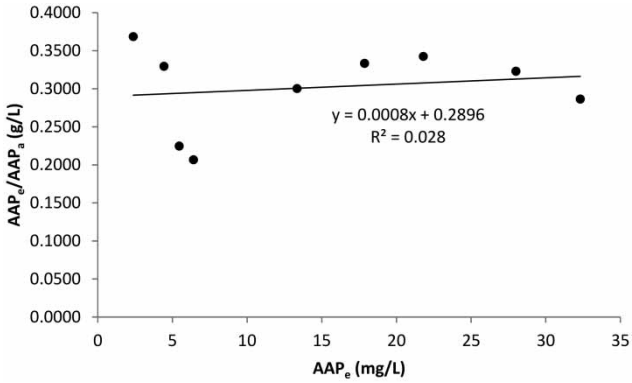

Figure 9 | Langmuir equilibrium plot.

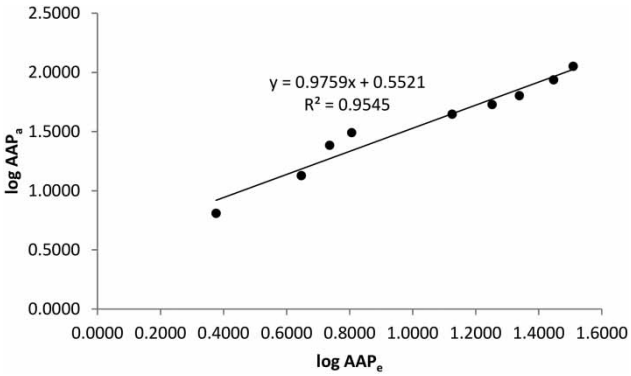

Figure 10 | Freundlich equilibrium plot.

The study of the influence of pH on the adsorption of AAP at pH range 3–8 (Figure 11) showed that the treatment efficiency initially increased from 66.12% at pH 2 to 77.33% at pH 4 after which the adsorption decreased to 63.22% at pH 8. The pH increase of the medium may have led to changes in the adsorbate structure and adsorbent properties thereby resulting in a decrease in the amount of AAP removed at pH 4–8. Bernal *et al.* (2017) reported that AAP (pKa = 9.5) coexist in both the ionized (a base) and non-ionised (an acid) forms. Thus, the distribution of acid and basic forms is strictly dependent on the solution pH and their interaction with solid may or may not favor the adsorption process if the forces of attraction or repulsion prevail, respectively.

The trend of Figure 12 indicates that the adsorption of AAP by the nano-TiO_2 decreased with the increase of temperature. This suggested that the nano-TiO_2 adsorption of AAP is exothermic. The adsorption of AAP by nano-TiO_2 at ambient temperature was 67.69% and decreased to about 43.89 at 343 K corresponding to 112.81 mg/g to 73.15 mg/g, respectively. The decrease of AAP adsorption capacity with the increase of AAP solution temperature might be due to desorption of the AAP molecules from the surface of nano-TiO_2 as the temperature increases. This is supported by Moussavi *et al.* (2016), who reported that the thermodynamic analysis of the adsorption of AAP onto a double-oxidized graphene oxide is exothermic.

The standard free energy (ΔG^o), enthalpy (ΔH^o), and entropy (ΔS^o) changes were calculated from Equations (7)–(9):

$$\Delta G^0 = -RT \ln K \tag{7}$$

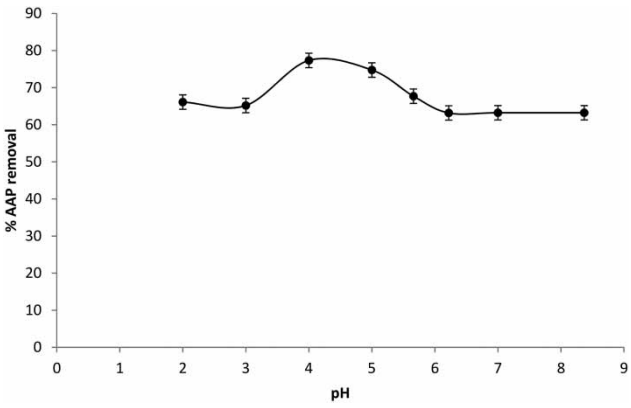

Figure 11 | Influence of pH. Experimental conditions: concentration of AAP: 100 mg/L; vol. of AAP aqueous solution: 50 mL; nano-TiO_2 dosage: 0.03 g; contact time: 60 min; stirring speed: 120 rpm; ambient temperature.

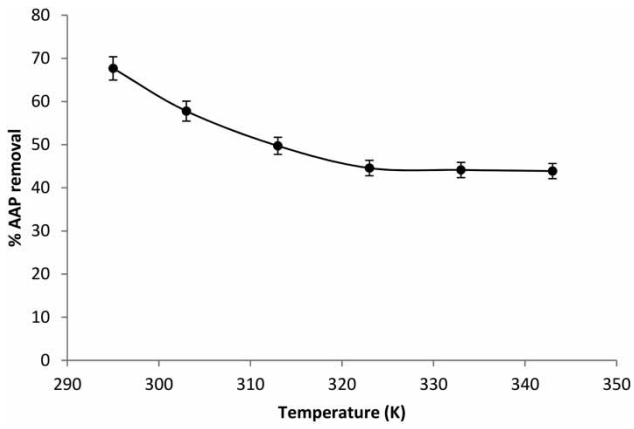

Figure 12 | Influence of temperature. Experimental conditions: concentration of AAP: 100 mg/L; vol. of AAP aqueous solution: 50 mL; nano-TiO_2 dosage: 0.03 g; contact time: 60 min; stirring speed: 120 rpm; pH of solution 5.66.

$$K = \frac{AAP_o - AAP_e}{AAP_e} \tag{8}$$

$$\log K = \frac{\Delta S^o}{2.303R} - \frac{\Delta H^o}{2.303RT} \tag{9}$$

where $AAP_o - AAP_e$ is the amount of the AAP adsorbed per liter, AAP_e is the equilibrium concentration of the solution in mg/L, T is temperature (K), R is ideal gas constant (8.314 J/mol/K), and K is thermodynamic equilibrium constant.

The Van't Hoff plot ($log\ K$ vs $1/T$) and thermodynamic parameters of AAP adsorption by nano-TiO_2 are presented in Figure 13 and Table 3, respectively. The calculated ΔH^o and ΔS^o of the adsorption of AAP by the nano-TiO_2 are −16.88 kJ/mol and −52.69 J/mol/K, respectively. The negative value of ΔG^o at 295 K and 303 K implies that the adsorption of AAP by nano-TiO_2 is spontaneous at these temperatures, but non-spontaneous at higher temperatures. The value of ΔG^o increased with the increase of AAP solution temperature, ΔH^o is negative, and K value decreased with the increase of temperature (Table 3). All these confirmed that the adsorption of AAP by nano-TiO_2 is exothermic under the selected conditions. The negative value of ΔS^o showed the decreased randomness of solid–liquid interphase during the treatment processes of AAP by the nano-TiO_2.

The experiments on the treatment of AAP by nano-TiO_2 have proven to be efficient and promising for the removal of AAP from contaminated water and wastewater.

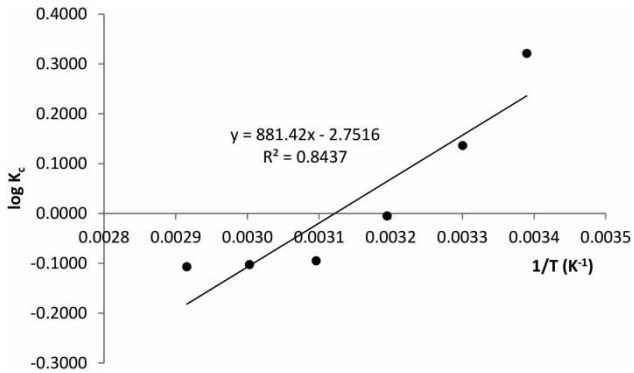

Figure 13 | Van't Hoff plot.

Table 3 | Thermodynamic parameters

T (K)	ΔH^o (kJ/mol)	ΔS^o (J/mol/K)	ΔG^o (J/mol)	K
295	− 16.88	− 52.69	−1,813.31	2.0945
303			−790.69	1.3687
313			29.26	0.9888
323			585.56	0.8041
333			653.21	0.7898
343			700.74	0.7821

Degradation capacity of AAP by ultrasound

The ultrasound degradation of 100 mL of 100 mg/L AAP (without pH adjustment (pH 5.66)) led to 53.84% removal efficiency. This prompted the need to investigate whether the change of pH of the AAP aqueous solution will enhance the degradation efficiency. Figure 14 shows that the rate of AAP degradation is strongly pH-dependent; the ultrasound treatment of AAP decreased as the pH of the solution increased from pH 3 to 8. This is supported by Im *et al.* (2014), who reported that the most favorable degradation pH of AAP is acidic. The hydrophobicity of AAP is favored at acidic conditions, thereby resulting in the accumulation of AAP (molecular form) at the interface of the cavitation bubbles, where a relatively higher concentration of $OH^{\cdot}$ is present (Villaroel *et al.* 2014). Ultrasonic degradation efficiency of approximately 57.43% and 53.78% were

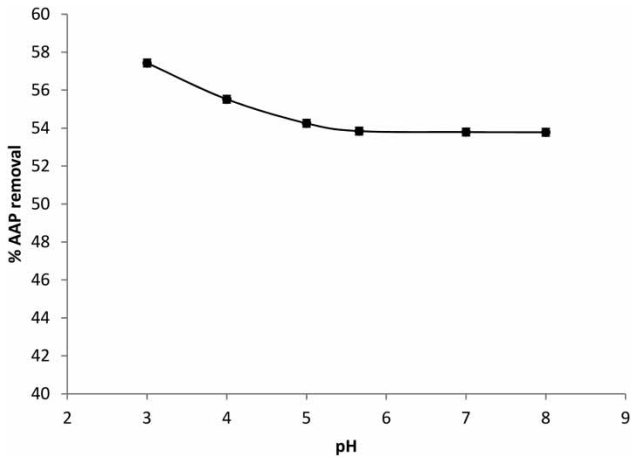

Figure 14 | Influence of pH on ultrasonic degradation. Experimental conditions: concentration of AAP: 100 mg/L; vol. of AAP aqueous solution: 100 mL; ultrasonic frequency: 20 kHz; time: 60 min; stirring speed: 180 rpm.

achieved at a pH of 3 and 8, respectively. A pH of 3 was maintained for further experiments.

Although a pH of 3 improved the ultrasound degradation of AAP (57.43%), the ultrasound treatment of AAP under normal condition (pH 5.66) should be encouraged (53.84%), due to the fact that the adjustment of solution pH is an additional cost and the discharge of the acidic resultant solution is hazardous to the environment.

The results on the influence of ultrasound time showed a rapid increase of the degradation of AAP from 12.30% at 10 min to 57.43% at 60 min sonication time (Figure 15(a)).

The degradation rate constant was determined by assuming a pseudo-first-order reaction kinetics (Equation (10)).

$$-\frac{dAAP}{dt} = kAAP \Leftrightarrow \ln\frac{AAP_o}{AAP_t} = kt \quad (10)$$

where AAP_o and AAP_t are AAP concentrations at time 0 and t, respectively, and k is the pseudo first-order rate constant.

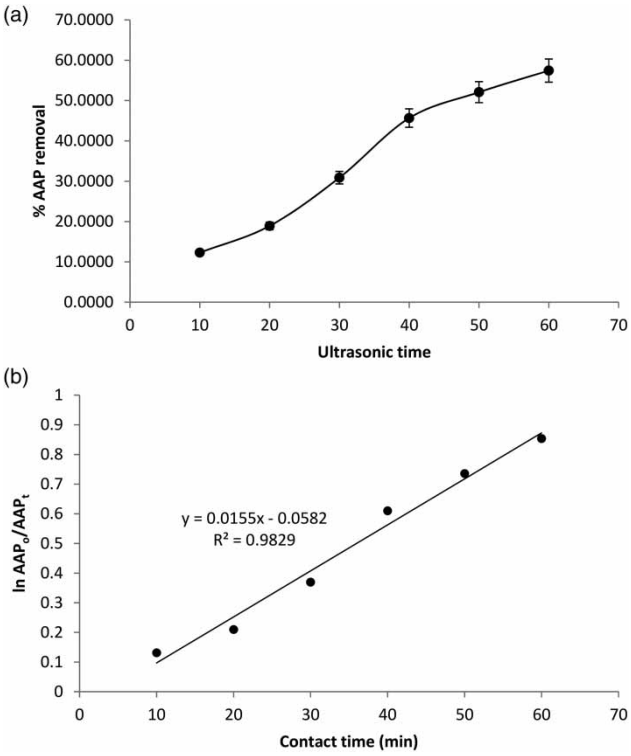

Figure 15 | (a) Influence of time on ultrasonic degradation: Experimental conditions: concentration of AAP: 100 mg/L; vol. of AAP aqueous solution: 100 mL; ultrasonic frequency: 20 kHz; pH: 3; stirring speed: 180 rpm. (b) Pseudo-first-order plot of AAP ultrasonic degradation.

A plot of $ln\ AAP_o/AAP_t$ against t (Figure 15(b)) was linear and k was obtained from the slope of the graph. The value obtained for the pseudo-first-order rate constant was $1.55 \times 10^{-2}\,min^{-1}$ and is similar to the study by Emery *et al.* (2005). The authors reported that the ultrasound degradation of pharmaceuticals obeys pseudo-first-order reaction kinetics.

The rate of ultrasound degradation of organic compounds usually depends on ultrasonic frequency. Moreover, there is the need to investigate the optimum frequency that will favor the degradation of pollutants. Thus, Figure 16 shows the percentage removal–frequency profiles of AAP during the ultrasound degradation of 100 mL of 100 mg/L AAP at a pH 3, contact time of 60 min, and a stirring speed of 180 rpm.

For the range of ultrasonic frequencies studied (20 kHz–100 kHz), the amount of AAP degradation decreased with the increase of the ultrasonic frequencies. This may be due to a reduced cavitational effect as ultrasonic frequency increased. The highest AAP removal was achieved with 20 kHz ultrasonic frequency. This finding is supported by Isariebel *et al.* (2009) and Im *et al.* (2014), who stated that the degradation of AAP decreased at higher ultrasonic frequencies. Im and co-workers attributed the lower degradation efficiency at a higher ultrasonic frequency to small bubble size and insufficient ultrasound reactions deriving from low collapse events.

In ultrasound degradation, AAP was degraded by reacting with $OH^{\cdot}$ which are generated from thermally dissociated water under ultrasound irradiation, while

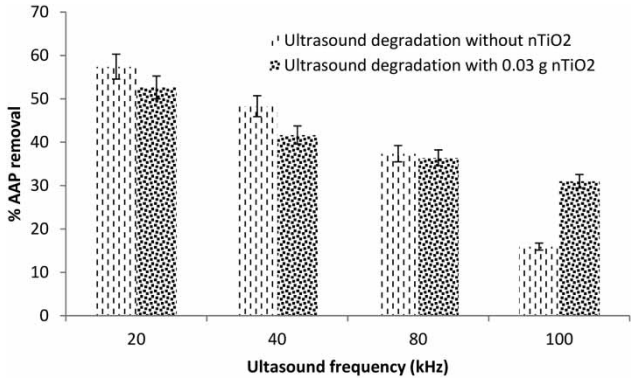

Figure 16 | Degradation efficiency by ultrasound with or without nano-TiO_2. Experimental conditions: concentration of AAP: 100 mg/L; vol. of AAP aqueous solution: 100 mL; pH: 3; time: 60 min; stirring speed: 180 rpm.

AAP molecules are adsorbed on the surface of nano-TiO_2 particles in the nano-TiO_2 treatment method. Researchers have suggested that the combination of adsorbents with ultrasound irradiation is suitable for the removal of persistent organic compounds and pharmaceuticals (Hamdaoui 2011; Zhao *et al.* 2011; Milenkovic *et al.* 2013). In our study, the addition of nano-TiO_2 into AAP aqueous solution improved the treatment efficiency for the nano-TiO_2/ultrasound treatment at 100 kHz but not for other ultrasound frequencies. At 100 kHz, 15.94% of AAP was degraded by ultrasound treatment and 40.01% of AAP was degraded by the combined nano-TiO_2/ultrasound treatment. However, approximately 52.61% of AAP was degraded by the use of ultrasound combined with nano-TiO_2, while 57.43% of AAP was degraded by the use of ultrasound without nano-TiO_2 when 100 mL of 100 mg/L AAP solution was sonicated for 60 min, at 20 kHz, and pH of 3. The application of all the optimum operating conditions to the remediation of AAP in a sequential approach showed that the degradation of AAP by ultrasound (20 kHz, pH 3, 60 min) followed by adsorption with nano-TiO_2 (0.03 g, 60 min) resulted in approximately 99.50% AAP removal efficiency.

This study has proven the effectiveness of ultrasound, nano-TiO_2, and the integrated treatment processes for the remediation of AAP or other emerging water and wastewater contaminants. Thus, we proposed a schematic diagram of a sequential nano oxides/ultrasound removal of pollutants from contaminated water or wastewater (Figure 17).

A comparison of the percentage removal of AAP using various techniques is listed in Table 4. The percentage removal of AAP by ultrasound, nano-TiO_2, and the integrated treatment processes in comparison with others' methods show satisfactory performance.

CONCLUSION

The extent of nano-TiO_2, ultrasound, and nano-TiO_2/ultrasound degradation of AAP was strongly influenced by the operating conditions, such as nano-TiO_2 dosage, contact time, initial AAP concentration, ultrasound frequency, pH, and temperature. The kinetics and equilibrium studies of AAP adsorption by the nano-TiO_2 followed the pseudo-second-order and Freundlich models, respectively. The thermodynamic parameters showed that the adsorption process is exothermic, spontaneous at 295 K and 303 K but non-spontaneous at higher temperatures. The optimum AAP removal efficiency achieved when 50 mL of 100 mg/L AAP solution was treated with 0.03 g nano-TiO_2 at 60 min contact time, 120 rpm, and pH 4 was 77.33%. Ultrasound treatment without the addition of nano-TiO_2 resulted in 57.43% degradation, whereas 52.61% degradation was achieved when nano-TiO_2 was mixed with AAP aqueous solution under ultrasound at a frequency of 20 kHz and pH 3. This investigation has shown that ultrasonic treatment alone or the addition of nano-TiO_2 into the AAP aqueous solution before sonolysis was not able to degrade AAP completely. However, the use of inline ultrasound degradation of

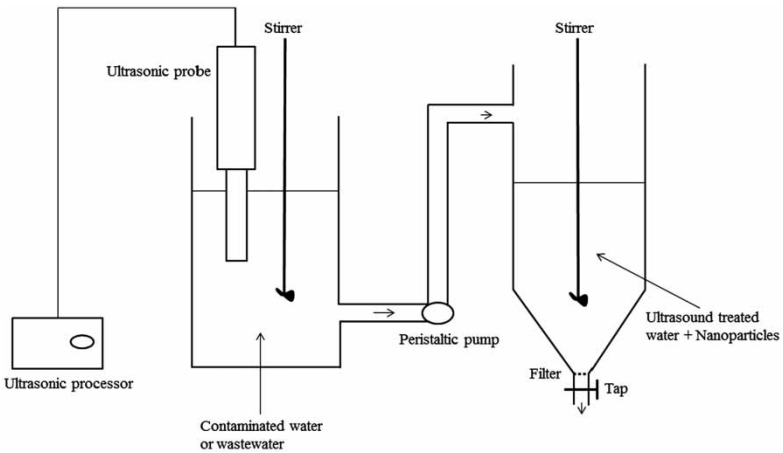

Figure 17 | Proposed schematic diagram of a sequential nano oxides/ultrasound degradation of pollutants.

Table 4 | Comparison of AAP removal percentage with the literature

Techniques	Percentage removal (%)	Reference
Ultrasound (100 mg/L AAP, 574 kHz)	70 (4 hours); 96 (8 hours)	Isariebel *et al.* (2009)
UV	<10	Aguilar *et al.* (2011)
UV + TiO_2 as catalyst	97	
Electrolysis with reticulated vitreous carbon (RVC) electrodes	90	Arredondo Valdez *et al.* (2012)
Electrolysis with modified TiO_2/RVC electrode	90	
Electrolysis with modified $CuO_2/TiO_2/Al_2O_3$/RVC electrode	98	
Electrolysis with modified TiO_2/RVC electrode + UV	95	
Electrolysis with modified $CuO_2/TiO_2/Al_2O_3$/RVC electrode + UV	99	
Chlorination (dose 49–54 mmol L^{-1}, pH 5.5, 24 h)	>95	Westerhoff *et al.* (2005)
Electrochemical oxidation (5.7 mA/cm^2, pH 3, 6 hr)	96	Zavala & Estrada (2016)
Double-oxidized graphene oxide as adsorbent	83	Moussavi *et al.* (2016)
Chemically treated chicken bone waste as adsorbent	93	Yusoff *et al.* (2017)
Ultrasound (100 mg/L AAP, 20 kHz, 60 min)	57.43	Our study
Nano-TiO_2 as adsorbent	77.33	
Combined ultrasound (20 kHz) and nano-TiO_2	52.61	
Sequential ultrasound (20 kHz) and nano-TiO_2	99.50	

AAP before nano-TiO_2 treatment effectively removed 99% AAP, showing that a sequential process had an additive effect whereas a simultaneous combined approach was not significantly effective.

ACKNOWLEDGEMENTS

The authors express thanks to the Vaal University of Technology, South Africa for granting a Postdoctoral Research Fund (PDRF) for this study.

REFERENCES

Aguilar, C. A., Montalvo, C., Ceron, J. G. & Moctezuma, E. 2011 Photocatalytic degradation of acetaminophen. *International Journal of Environmental Research* **5**, 1071–1078.

Andreozzi, R., Caprio, V., Marotta, R. & Vogna, D. 2003 Paracetamol oxidation from aqueous solutions by means of ozonation and H_2O_2/UV system. *Water Research* **37**, 993–1004.

Arredondo Valdez, H. C., García Jiménez, G., Gutiérrez Granados, S. & Ponce de León, C. 2012 Degradation of paracetamol by advance oxidation processes using modified reticulated vitreous carbon electrodes with TiO_2 and CuO/TiO_2/Al_2O_3. *Chemosphere* **89**, 1195–1201.

Basavaraju, M., Mahamood, S., Vittal, H. & Shrihari, S. 2011 A novel catalytic route to degrade paracetamol by Fenton process. *International Journal of Research in Chemistry and Environment* **1**, 157–164.

Bernal, V., Erto, A., Giraldo, L. & Moreno-Piraján, J. C. 2017 Effect of solution pH on the adsorption of paracetamol on chemically modified activated carbons. *Molecules* **22**, 1032. doi:10.3390/molecules22071032.

Chen, H., Gao, B. & Li, H. 2015 Removal of sulfamethoxazole and ciprofloxacin from aqueous solutions by graphene oxide. *Journal of Hazardous Materials* **282**, 201–207.

Emery, R., Papadakia, M., Freitas dos Santos, L. & Mantzavinos, D. 2005 Extent of sonochemical degradation and change of toxicity of a pharmaceutical precursor (triphenylphosphine oxide) in water as a function of treatment conditions. *Environment International* **31**, 207–211.

Galhetas, M., Mestre, A. S., Pinto, M. L., Gulyurtlu, I., Lopes, H. & Carvalho, A. P. 2014 Carbon-based materials prepared from pine gasification residues for acetaminophen adsorption. *Chemical Engineering Journal* **240**, 344–351.

Gomez, M. J., Bueno, M. J. M., Lacorte, S., Fernandez-Alba, A. R. & Aguera, A. 2007 Pilot survey monitoring pharmaceuticals and related compounds in a sewage treatment plant located on the Mediterranean coast. *Chemosphere* **66**, 993–1002.

Gros, M., Petrovic, M. & Barcelo, D. 2006 Development of a multiresidue analytical methodology based on liquid chromatography-tandem mass spectrometry (LC-MS/MS) for

screening and trace level determination of pharmaceuticals in surface and wastewaters. *Talanta* **70**, 678–690.

Haider, A. J., Jameel, Z. N. & Taha, S. Y. 2015 Synthesis and characterization of TiO_2 nanoparticles via sol-gel method by pulse laser ablation. *Engineering Technology Journal* **33**, 761–771.

Hamdaoui, O. 2011 Intensification of the sorption of Rhodamine B from aqueous phase by loquat seeds using ultrasound. *Desalination* **271**, 279–286.

Hiremath, D. C., Hiremath, C. V. & Nandibewoor, S. T. 2006 Oxidation of paracetamol drug by a new oxidant diperiodatoargentate (III) in aqueous alkaline medium. *E-Journal of Chemistry* **3**, 13–24.

Im, J. K., Boateng, L. K., Flora, J. R. V., Her, N., Zoh, K. D., Son, A. & Yoon, Y. 2014 Enhanced ultrasonic degradation of AAP and naproxen in the presence of powdered activated carbon and biochar adsorbents. *Separation and Purification Technology* **123**, 96–105.

Isariebel, Q. P., Carine, J. L., Ulises-Javier, J. H., Anne-Marie, W. & Henri, D. 2009 Sonolysis of levodopa and paracetamol in aqueous solutions. *Ultrasonics Sonochemistry* **16**, 610–616.

Milenkovic, D., Bojic, A. L. & Veljkovic, V. 2013 Ultrasound-assisted adsorption of 4-dodecylbenzene sulfonate from aqueous solutions by corn cob activated carbon. *Ultrasonics Sonochemistry* **20**, 955–962.

Moussavi, G., Hossaini, Z. & Pourakbar, M. 2016 High-rate adsorption of acetaminophen from the contaminated water onto double-oxidized graphene oxide. *Chemical Engineering Journal* **287**, 665–673.

Pettibone, J. M., Cwiertny, D. M., Scherer, M. & Vicki, H. 2008 Grassian adsorption of organic acids on tio_2 nanoparticles: effects of pH, nanoparticle size, and nanoparticle aggregation. *Langmuir* **24**, 6659–6667.

Ratpukdi, T. 2014 Degradation of paracetamol and norfloxacin in the aqueous solution using vacuum ultraviolet (VUV) process. *Journal of Clean Energy Technologies* **2**, 168–170.

Stackelberg, P. E., Furlong, E. T., Meyer, M. T., Zaugg, S. D., Henderson, A. K. & Reissman, D. B. 2004 Persistence of pharmaceutical compounds and other organic wastewater contaminants in a conventional drinking water treatment plant. *Science of the Total Environment* **329**, 99–113.

Ternes, T. A. 1998 Occurrence of drugs in German sewage treatment plants and rivers. *Water Research* **32**, 3245–3260.

Vijayalakshmi, R. & Rajendran, V. 2012 Synthesis and characterization of nano-tio_2 via different methods. *Archives of Applied Science Research* **4**, 1183–1190.

Villaroel, E., Silva-Agredo, J., Petrier, C., Taborda, G. & Torres-Palma, R. A. 2014 Ultrasonic degradation of acetaminophen in water: effect of sonochemical parameters and water matrix. *Ultrasonics Sonochemistry* **21**, 1763–1769.

Westerhoff, P., Yoon, Y., Shane, S. & Wert, E. 2005 Fate of endocrine-disruptor, pharmaceutical, and personal care product chemicals during simulated drinking water treatment processes. *Environmental Science and Technology* **39**, 6649–6663.

Xagoraraki, I., Hullman, R., Song, W., Li, H. & Voice, T. 2008 Effect of pH on degradation of acetaminophen and production of 1,4-benzoquinone in water chlorination. *Journal of Water Supply: Research and Technology-AQUA* **57**, 381–390.

Yang, L., Yu, L. E. & Ray, M. B. 2009 Photocatalytic oxidation of paracetamol: dominant reactants, intermediates, and reaction mechanisms. *Environmental Science & Technology* **43**, 460–465.

Yusoff, N. A., Ngadi, N., Alias, H. & Jusoh, M. 2017 Chemically treated chicken bone waste as an efficient adsorbent for removal of acetaminophen. *Chemical Engineering Transactions* **56**, 925–930.

Zavala, M. A. L. & Estrada, E. E. 2016 Degradation of acetaminophen and its transformation products in aqueous solutions by using an electrochemical oxidation cell with stainless steel electrodes. *Water* **8**, 383. doi:10.3390/w8090383.

Zhao, D., Cheng, J., Vecitis, C. D. & Hoffmann, M. R. 2011 Sorption of perfluorochemicals to granular activated carbon in the presence of ultrasound. *Journal of Physical Chemistry A* **115**, 2250–2257.

First received 7 July 2017; accepted in revised form 23 August 2017. Available online 16 October 2017